J Radioanal Nucl Chem (2012) 292:745–750
DOI 10.1007/s10967-012-1646-9

Measurement of reaction cross-sections for ^{64}Ni(n, γ) ^{65}Ni at E_n = 0.025 eV and ^{58}Ni(n, p) ^{58}Co at E_n = 3.7 MeV

B. S. Shivashankar · H. Naik · S. V. Suryanarayana · P. M. Prajapati · V. K. Mulik · K. C. Jagadeesan · S. V. Thakare · A. Goswami · S. Ganesan

Received: 5 October 2011 / Published online: 5 February 2012

Abstract The reaction cross-sections for ^{64}Ni(n, γ) ^{65}Ni at E_n = 0.025 eV and ^{58}Ni (n, p) ^{58}Co at E_n = 3.7 MeV have been experimentally determined using activation and off-line γ-ray spectrometric technique. The thermal neutron flux used is from the thermal Column of the reactor APSARA at BARC, Mumbai, whereas the neutron energy of 3.7 MeV is from the ^{7}Li(p, n) reaction at Pelletron facility, TIFR, Mumbai. The ^{64}Ni(n, γ) ^{65}Ni and ^{58}Ni(n, p) ^{58}Co reactions cross-sections from present work are compared with the available literature data and found to be in good agreement. The ^{58}Ni(n, p) ^{58}Co reaction as a function of neutron energy is also calculated theoretically using TALYS computer code version 1.2 and found to be higher than the experimental data.

Keywords ^{64}Ni(n, γ) ^{65}Ni reaction cross-section · E_n = 0.025 eV · ^{58}Ni (n, p) ^{58}Co reaction cross-section · E_n = 3.7 MeV · Activation technique · Off-line γ-ray spectrometry · TALYS calculation

B. S. Shivashankar
Department of Statistics, Manipal University, Manipal 576104, India

H. Naik (✉) · A. Goswami
Radiochemistry Division, Bhabha Atomic Research Center, Mumbai 400 085, India
e-mail: naikhbarc@yahoo.com

S. V. Suryanarayana
Nuclear Physics Division, Bhabha Atomic Research Center, Mumbai 400 085, India

P. M. Prajapati
M S University of Baroda, Vadodara 390 002, India

V. K. Mulik
Department of Physics, University of Pune, 411 007 Pune, India

K. C. Jagadeesan · S. V. Thakare
Radiopharmaceutical Division, Bhabha Atomic Research Center, Mumbai 400 085, India

S. Ganesan
Reactor Physics Design Division, Bhabha Atomic Research Center, Mumbai 400 085, India

Introduction

Nuclear data on neutron induced reaction cross-section of structural material such as Zr, Nb, stainless steel and Al are important from reactor point of view. This is because in thermal reactors zircaloy-2 is used as the cladding material and Zr–2.5% Nb as structural material for coolant tube of the fuel [1]. On the other hand stainless steel is used as the cladding material in the fast rector [2–4]. Besides this, stainless steel is used as the calandria vessel and pipe lines of secondary coolant circuit. In stainless steel Ni is one of the component with isotopic composition ^{58}Ni(68.077%), ^{60}Ni(26.223%), ^{61}Ni(1.140%), ^{62}Ni(3.634%), ^{64}Ni(0.926%) respectively. In reactor there is a broad neutron spectrum of energy ranging from 0 to 10 MeV [5]. However, in the fast reactor, the neutron energy is on the higher side i.e. from 10 to 15 MeV. So it is worth while to determine the different reaction cross section of Ni with different mono energetic neutrons.

Sufficient ^{64}Ni(n, γ)^{65}Ni reaction cross section data are available in literature at thermal neutron energy [6–11] and neutron energy higher than 0.52 keV [12–16]. However, the available data determined earlier at thermal neutron energy are based on the technique such as γ-ray counting using G–M counter [6], prompt γ-ray coincidence counting using $4\pi\beta$–γ counter and NaI(Tl) detector [7, 8] or by using

Ge(Li) and NaI(Tl) detector [10, 11]. The activation technique and off-line γ-ray spectrometry used by Gleason et al. [9] was based on the neutron source ^{252}Cf(SF), which is having neutron spectrum. Similarly, the ^{64}Ni(n, γ)^{65}Ni reaction cross section at neutron energy higher than 0.52 keV are also determined using activation [12–15] and neutron time of flight [16] technique. From all these data it can be seen that the ^{64}Ni(n, γ)^{65}Ni reaction cross-section for thermal and higher energy neutron has a large variation. Similarly, the ^{58}Ni (n, p)^{58}Co reaction cross-section at various mono-energetic neutrons are also available in literature [17–32] based on activation and off-line γ-ray spectroscopic technique. However, most of the ^{58}Ni (n, p)^{58}Co reaction cross-section data are based on the neutron energy from $D + D$ or $D + T$ reaction except the some data based on the neutron energy from $P + T$ [21, 22, 25] and ^{7}Li(p, n)^{7}Be reactions [19, 20, 23]. Besides this, most of the earlier data are based on activation technique followed by γ-ray counting by NaI(Tl) detector [17–20]. On the other hand the γ-ray measurements with Ge(Li) or HPGe detector [21–32] has been carried out to determine the ^{58}Ni (n, p)^{58}Co reaction cross-section. From all these data it can be seen that the ^{58}Ni (n, p)^{58}Co reaction cross-section data has large variation between the neutron energy of 3–5 and 12–18 MeV.

In the present work, we have determined the reaction cross-sections for ^{64}Ni(n, γ)^{65}Ni at thermal neutron energy and for ^{58}Ni (n, p)^{58}Co at mono-energetic neutrons of 3.7 MeV using activation and off-line γ-ray spectroscopic technique. The mono-energetic neutron beam for thermal neutron used was from the thermal column of the reactor APSARA, BARC at Mumbai, whereas the 3.7 MeV neutron was obtained from the ^{7}Li (p, n)^{7}Be reaction using 5.5 MeV proton beam at BARC-TIFR Pelletron facility at TIFR, Mumbai.

Experimental methods

The measurement of neutron-induced reaction cross-sections for nickel isotopes were carried out using two separate irradiations. First one is for thermal neutron irradiation of ^{64}Ni(n, γ)^{65}Ni reaction at APSARA reactor and second one is for ^{58}Ni(n, p)^{58}Co reaction at BARC-TIFR Pelletron facility, Mumbai, India. Details of experimental procedure applied to measure the neutron cross-sections for the two different irradiations are given below.

Thermal neutron activation cross-sections measurements of ^{64}Ni (n, γ)^{65}Ni

A known amount (0.1435 g) of natural Ni metal foil of thickness about 1 mm and Au metal foil (0.0218 g) of thickness 0.1225 mm for neutron flux monitor were wrapped separately with 0.025 mm thick super pure aluminum foil and doubly sealed with alkathene bags. These samples were kept inside an irradiation capsule made of polypropylene. The capsule containing samples were doubly sealed with alkathene bags and were taken for irradiation. These samples were irradiated in the thermal column of the light water moderated highly enriched uranium fuelled swimming pool APSARA reactor [5] for the period of 6 h and 30 min. After sufficient cooling, the irradiated samples of Ni and Au along with Al wrapper were mounted on two different perspex plates and taken for γ-ray spectrometry. Radioactivity in the irradiated Ni and Au samples were measured using energy and efficiency calibrated 80 cm^3 high-purity germanium (HPGe) detector coupled to a PC-based 4 K multi-channel analyzer in live time mode. The efficiency of the detector was 20% with energy resolution of 2.0 keV FWHM at 1332.0 keV peak of ^{60}Co. The standard ^{152}Eu source having γ-rays in the energy range of 121.8–1408 keV was used for energy and efficiency calibration. The dead time of the detector system during counting was always kept less than 5% by placing the sample at a suitable distance to avoid pile up effects. A typical γ-ray spectrum of the thermal neutron irradiated nickel sample is shown in Fig. 1. The γ-ray spectrum was analyzed with PHAST peak fitting program (Mukhopadhyaya PK, 2001, Personal communication), which can search for up to 500 peaks and fit model peak shape. Measured disintegration rates, based on the γ-ray energies of 811 keV for ^{65}Ni confirmed that no interfering activities were present. The radioactive decay of the samples was followed to confirm the identity of nuclide being studied.

Measurement of ^{58}Ni(n, p)^{58}Mn reaction cross-section at average $E_n = 3.7$ MeV

The experiment was carried out using 14 UD BARC-TIFR Pelletron facilities at Mumbai, India. The neutron beam was produced from the ^{7}Li(p, n)^{7}Be reaction [33] at six

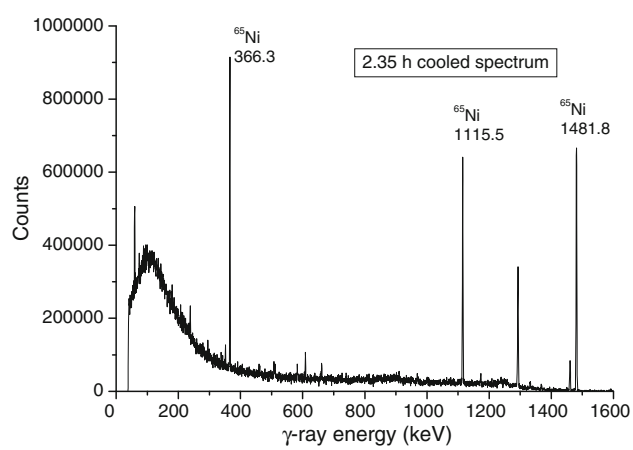

Fig. 1 γ-ray spectrum of ^{65}Ni from ^{64}Ni(n, γ) reaction in the thermal neutron irradiated nickel sample

meter height main line above the analyzing magnet to utilize the maximum proton current from the accelerator. The lithium foil was made of natural lithium of thickness 3.7 mg/cm^2 and wrapped with tantalum foil. The front tantalum foil facing the proton beam was of thickness 3.9 mg/cm^2, in which degradation of proton energy was only 30 keV. On the other hand, the back tantalum foil was of 1 mm thick to stop the proton beam. A known amount (0.1448 g) of natural nickel with ^{58}Ni (68.077%) and 0.1556 g of natural indium metal foil were wrapped separately with 0.025 mm thick Al foil. The size of the Ni–In stacked was 4 mm × 4 mm. Then a stacked was made from these two targets, which were additionally wrapped with additional Al foil of 0.025 mm thick. The Ni–In stack sample was mounted at zero degree with respect to beam direction at a distance of 2.1 cm from the location of the Ta–Li–Ta stack. A schematic diagram for this experimental setup is shown in Fig. 2. The stack of Ni–In sample was irradiated for 6 h with the neutrons generated from ^{7}Li(p, n)^{7}Be reaction using proton beam of 5.5 MeV. The proton current during the irradiation was 100 nA. The average neutron energy for 5.5 MeV proton beam was calculated as 3.7 ± 0.3 MeV. The neutron spectrum from ^{7}Li(p, n)^{7}Be reaction corresponding to proton energy of 5.5 MeV is shown in Fig. 3. The detailed calculation of average neutron energy was given in Ref. [34]. The irradiated samples Ni and In along with Al wrapper were cooled for 2 h, mounted on two different perspex plates and taken for γ-ray spectrometry as mentioned in section II A. A typical γ-ray spectrum of the nickel sample from 3.7 ± 0.3 MeV neutron irradiation is shown in Fig. 4. The γ-ray spectra were analyzed using PHAST peak fitting program.

Calculations and results

Calculations of neutron flux

In the case of thermal neutron activation cross-section measurements, the photo-peak activity of 411.8 keV γ-line

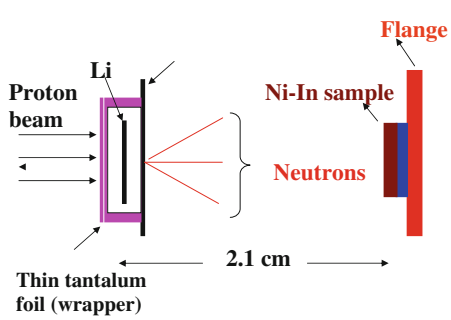

Fig. 2 Schematic diagram showing the arrangement used for neutron irradiation using Li(p, n)^{7}Be reaction

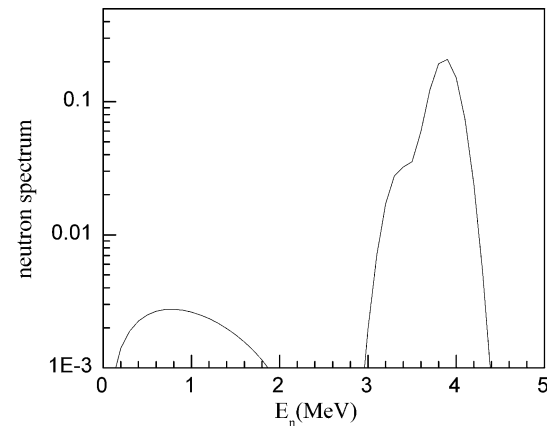

Fig. 3 Neutron spectrum for ^{7}Li(p, n) reaction at E_p = 5.5 MeV from Ref. [34]

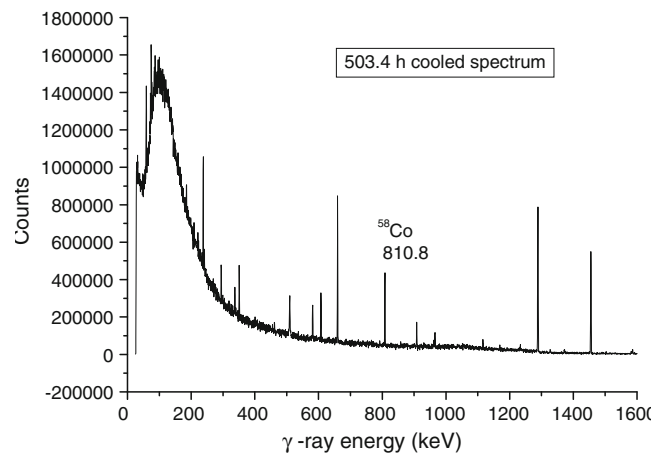

Fig. 4 γ-ray spectrum of ^{58}Co from ^{58}Ni(n, p) reaction in the 3.7 MeV neutron irradiated nickel sample

of ^{198}Au from the Au^{197}Au(n, γ) reaction was used for flux determination. At higher neutron energy of 3.7 MeV, the photo-peak activity of 336.24 keV γ-lines of ^{115}In^m from the ^{115}In(n, n') reaction was used as a flux monitor. The observed photo-peak activity of γ-line was related to neutron flux (Φ) with the relation as given below,

$$A_{\mathrm{obs}}(CL/LT) = N\sigma\Phi a\varepsilon(1-\exp(-\lambda t))\exp(-\lambda T)(1-\exp(-\lambda CL))/\lambda \quad (1)$$

where N is the number of target atoms and σ is the monitor reaction cross-section. 'a' is the branching intensity of γ-lines and ε is its detection efficiency. 't', T, CL and LT are the irradiation time, cooling time, clock time and counting time respectively.

The observed photo-peak activities of 411.8 keV of ^{198}Au and 336.24 keV of ^{115}In^m lines were obtained using PHAST peak fitting program (Mukhopadhyaya PK, 2001, Personal communication). By taking the standard cross-sections (σ) values from Ref. [35], neutron flux was calculated separately for two different irradiations. The

Table 1 Nuclear spectroscopic data

Nuclide	Half life	γ-ray energy (keV)	γ-ray abundance (%)
^{198}Au	2.272 d	411.80	95.62
^{115}In^{m}	4.486 h	336.24	45.8
^{65}Ni	2.5172 h	1481.84	24.0
^{58}Co	70.86 d	810.775	99.0

nuclear spectroscopic data such as half-life, γ-ray energy, branching intensity were taken from NuDat [36] (BNL, U.S.A) and are given in Table 1. Using Eq. 1, we have calculated neutron flux as 1.105×10^8 n cm^{-2} s^{-1}and 1.1×10^7 n cm^{-2} s^{-1} for the thermal neutron energies (0.0253 eV) and 3.7 MeV respectively.

Calculations of neutron cross-sections

The nuclear data used for the calculation of ^{64}Ni(n, γ)^{65}Ni and ^{58}Ni(n, p)^{58}Co reaction cross-sections were taken from NuDat (BNL, USA). From the observed photo-peak activity of 1481.84 keV γ-line of ^{65}Ni ($T_{1/2} = 2.5172$ h), ^{64}Ni(n, γ)^{65}Ni cross-section was calculated at thermal neutron energy using the same decay Eq. 1 with modified form given below

$$\sigma = \frac{A_{\mathrm{obs}}(CL/LT)\lambda}{N\Phi a\varepsilon(1-\exp(-\lambda t))\exp(-\lambda T)(1-\exp(\lambda CL))} \quad (2)$$

All the terms in Eq. 2 has the same meaning as in the Eq. 1. In Eq. 2, the observed photo-peak activity of 810.775 keV γ-line of ^{58}Co ($T_{1/2} = 70.78$) was used to calculate ^{58}Ni(n, p)^{58}Co reaction cross-section at neutron energy of 3.7 MeV. The observed photo-peak activities of corresponding γ-lines of ^{65}Ni and ^{58}Co were obtained by using PHAST peak fitting program (Mukhopadhyaya PK, 2001, Personal communication).

The ^{64}Ni(n, γ)^{65}Ni and ^{58}Ni(n, p)^{58}Co reaction cross-sections determined in the present work at neutron energies of 0.025 eV and 3.7 ± 0.3 MeV are given in the Table 2. The uncertainties shown in the measured neutron reaction cross-sections are the precision values from two measurements. The overall uncertainty represents contribution from both random and systematic errors. The random error in the observed activity is primarily due to the counting statistics and is estimated to be 10–15%, which can be determined by accumulating the data for an optimum time period that depends on the half-life of the nuclides of interest. On the other hand, the systematic error is due to uncertainties in the irradiation time (~2%), in the detection efficiency calibration (~3%), in the half-life of the reaction products and in the γ-ray abundances (~2%). The overall systematic error is about 4%. The overall uncertainty for the cross-section is obtained about 11–16%.

Discussion and conclusion

It can be seen from Table 2 that the ^{64}Ni(n, γ)^{65}Ni reaction cross-section at thermal neutron energy from the present work is in agreement with the literature data [6–11], which shows the correctness of the present approach. In order to examine this, the ^{64}Ni(n, γ)^{65}Ni reaction cross-section from thermal neutron energy to 5 MeV from Refs. [6–16] has been plotted in Fig. 5. It can be seen from the Fig. 5 that the present experimental data for thermal neutron energy agrees very well with the literature data. However, the present data is more reliable due to the use of exact thermal neutron flux in the thermal Column of the reactor APSARA and activation technique followed by off line γ-ray spectrometric technique using HPGe detector. Further, it can be seen from Fig. 5 that the ^{64}Ni(n, γ)^{65}Ni reaction cross-section decreases with increase of neutron energy, which is a general feature of the neutron capture cross-section due to opening up of other reaction channels such as (n, n'), (n, α) and (n, p) etc.

It can be also seen from Table 2 that the ^{58}Ni(n, p)^{58}Co reaction cross-section at neutron energy of 3.7 MeV is in good agreement with the literature data [17–20, 25] and is more reliable due to the use of similar technique and

Table 2 Experimentally measured neutron cross-sections (σ) of Ni isotopes

Energy	Reaction	σ (mb)	IAEA-EXFOR (mb)	JENDL 4.0 (mb)	ENDF/B-VII (mb)	TENDL 2010 (mb)
Thermal	^{64}Ni(n, γ)^{65}Ni	1590 ± 20	1600[a]	1480	1518	1620.4
			1960[b]			
3.7 ± 0.3 MeV	^{58}Ni(n, p)^{58}Co	317 ± 36	311.8[c]	254–321[f]	275–356[g]	296–328[h]
			332.8[d]			
			380.7[e]			

[a,b] The cross-section at thermal neutron energy, taken from [6] and [11] respectively

[c,d,e] The cross-section is for $E_n = 3.641$, 3.711 and 4.008 MeV respectively, taken from [23]

[f] The cross-section is for range of neutron energy of 3–4 MeV

[g] The cross-section is for range of neutron energy of 3.5–4 MeV

[h] The cross-section is for range of neutron energy of 3.6–3.8 MeV

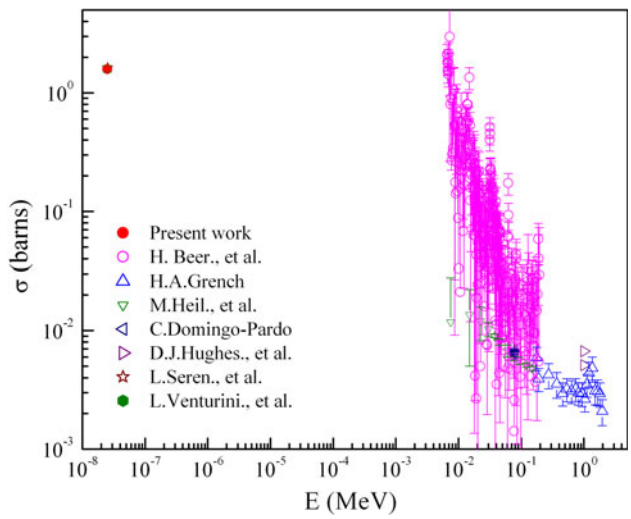

Fig. 5 Plot of $^{64}Ni(n, \gamma)^{65}Ni$ reaction cross-section as a function neutron energy

mono-energetic neutron source from $^{7}Li(p, n)^{7}Be$ reaction. The present data along with literature data from Refs. [17–32], are plotted in Fig. 6 as a function of neutron energy for comparison. It can be seen from Fig. 2 that the $^{58}Ni(n, p)^{58}Co$ reaction cross-section increases with neutron energy up to 7.5 MeV. Then it remains almost constant up to neutron energy of 11 MeV and there after it decrease due to the opening of other reaction channels. In order to examine this the $^{58}Ni(n, p)^{58}Co$ reaction cross-section as a function of neutron energy was calculated theoretically using computer code TALYS 1.2 [37].

TALYS [37] is a computer code for the prediction and analysis of nuclear reactions that involve photons, neutrons, protons, deuterons, tritons, hellions and alpha particles, in the energy range of 1 keV to 200 MeV and for target nuclides of masses 12 and heavier. For this, TALYS integrates the optical model, direct, pre-equilibrium, fission and statistical nuclear reaction models in one calculation scheme and thereby gives a prediction for all the open reaction channels. In TALYS, several options are included for the choice of different parameters such as γ-strength functions, nuclear level densities and nuclear model parameters etc. In the present work, we calculated neutron-induced reaction cross-sections of ^{58}Ni target using the default option in the TALYS code [37]. All possible outgoing channels for the given photon energy were considered. However, the cross-section for the (n, p) reaction was specially looked for and collected. The $^{58}Ni(n, p)^{58}Co$ reaction cross-section as a function of neutron energy from TALYS [37] are also plotted in Fig. 6. It can be seen from Fig. 6 that $^{58}Ni(n, p)^{58}Co$ reaction cross-section from TALYS 1.2 is in agreement with the experimental data from the present work and from Refs. [21–32, 38], which shows correctness of the present approach.

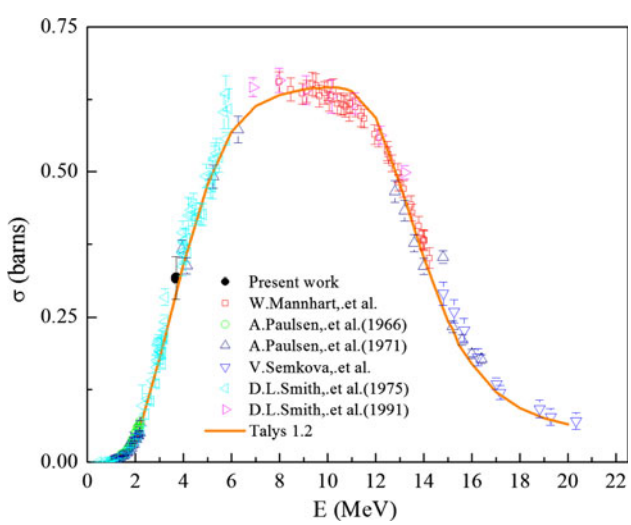

Fig. 6 Plot of $^{58}Ni(n, p)^{58}Co$ reaction cross-section as a function neutron energy

From the above discussion it can be said that, (i) in the present work the reaction cross-section $^{64}Ni(n, \gamma)^{65}Ni$ at thermal neutron energy and $^{58}Ni(n, p)^{58}Co$ at 3.7 MeV are determined using activation and off-line γ-ray spectrometry, which are in good agreement with the literature data. (ii) The $^{58}Ni(n, p)^{58}Co$ reaction cross-section as a function of neutron energy was also calculated theoretically using computer code TALYS 1.2 and are found to be in agreement with the experimental data from the literature and present work.

Acknowledgments The authors are thankful to the staff of APSARA reactor and TIFR-BARC Pelletron facility for their kind co-operation during experiment. We are also thankful to Mr. Ajit Mahadakar and Mrs. Dipa Thapa from target laboratory of Pelletron facility at TIFR, Mumbai for providing us the Li and Ta targets. One of the author Mr. B.S. Shivashankar gratefully acknowledge DAE-BRNS, Mumbai for the financial support.

References

1. Howe-Grant M (ed) (1996) Encyclopedia of chemical technology, vol 17, 4th edn. John & Sons, Inc, USA
2. IAEA-TECDOC–1319: thorium fuel utilization: options and trends. Fast reactors and accelerator driven systems knowledge base. Proceedings of three IAEA meetings held in Vienna in 1997, 1998 and 1999, November 2002. International Atomic Energy Agency, Vienna (Austria). http://www.iaea.org/inisnkm/nkm/aws/fnss/abstracts/abst_te_1319_web.html. Accessed 24 Jan 2012
3. Nuttin A, Heuer D, Billebaud A, Brissot R, Le Brun C, Liatard E, Loiseaux JM, Mathieu L, Meplan O, Merle-Lucotte E, Nifenecker H, Perdu F, David S (2005) Proc. Nucl. Energy 46:77
4. Allen TR, Crawford DC (2007) Science and technology of nuclear installations. Article ID 97486
5. Naik H, Nair AGC, Kalsi PC, Pandey AK, Singh RJ, Ramaswami A, Iyer RH (1996) Radiochim Acta 75:51
6. Seren L, Friedlander HN, Turkel SH (1947) Phys Rev 72:888

7. Lyon WS (1960) Nucl. Sci. Eng. 8:378
8. Ryves TB (1970) J. Nucl. Energy 24:35
9. Gleason G (1975) J. Radiochemical and Radioanalytical Lett. 23:317
10. Ishaq AFM, Robertson A, Prestwich WV, Kennett TJ (1977) Z. Phys. A 281:365
11. Venturini L, Pecequilo BRS (1997) Appl. Radiat. Isotope 48:493
12. Hughes DJ, Spatz WDB, Goldstein N (1949) Phys Rev 75:1781
13. Grench HA (1965) Phys Rev 140:B1277
14. Beer H, Spencer RR (1975) Nucl Phys A 240:29
15. Heil M, Käppeler F, Uberseder E (2008) Phys. Rev. C 77:015808
16. Domingo-Pardo C, Dillmann L, Faestermann T et al (2009) In: Conference proceedings. Am Inst Phys No. 1090, p 230
17. Gonzalez L, Rapaport J, Van Loef JJ (1960) Phys Rev 120:1319
18. Barry JF (1962) J. Nucl. Energy. AB 16:467
19. Konijn J, Lauber A (1963) Nucl. Phys. 48:191
20. Meadows JJ, Whalen JF (1963) Phys Rev 130:2022
21. Paulsen A, Liskien H (1966) C,66PARIS,217,6610, Nuclear Data For Reactors Conference, Paris 1966, p 217. http://www-nds.iaea.org/exfor/servlet/X4sGetInfo?subID=21741004&pointer=. Accessed 24 Jan 2012
22. Paulsen A, Widera R (1971) C,71CANT,129,7109, Chemical Nucl. Data Conference, Canterbury 1971, p 129. http://www-nds.iaea.org/exfor/servlet/X4sGetInfo?subID=20396004&pointer=. Accessed 24 Jan 2012
23. Smith DL, Meadows JW (1975) Nucl. Sci. Eng. 58:314
24. Hudson CG et al (1978) Ann Nucl Energy 5:589
25. Smith DL, Meadows JW, Vonach H, Wagner M, Haight RC, Mannhart W (1991) C,91JUELIC,282,9105, Conference on Nucl. Data for Sci. and Technol., Juelich 1991, p 282. http://www-nds.iaea.org/exfor/servlet/X4sGetInfo?subID=13513002&pointer=. Accessed 24 Jan 2012
26. Buczko GM, Csikai J, Sudar S, Grallert A, Jonah SA, Jimba BW, Chimoye T, Wager M (1995) Phys Rev C52:1940
27. Cezar Suita J, Gerbasi da silva A, Telmo Auler L, De Barros S (1997) Nucl Sci Eng 126:101
28. Avrigeanu V, Sudar S, Buczko CsM, Csikai J, Filatenkov AA, Chuvaev SV, DocZi R, Semkova V, Zelenetsky VA (1999) Phys Rev C 60:017602
29. Huang X, Weixiang Yu, Han X, Zhao W, Hanlin L, Chen J, Shi Z, Tang G, Zhang G (1999) Nucl. Sci. Eng. 131:267
30. Shimizu T, Sakane H, Shibata M, Kawade K, Nishitani T (2004) Nucl. Energy 31:975
31. Semkova V, Avrigeanu V, Glodariu T, Plompen AJM, Reimer P, Smith DL, Sudar S, Koning A, Forrest R (2004) Nucl Phys A 730:255
32. Mannhart W, Schmidt D (2007) Rep. PTB-N-53
33. Masnhnik SG, Chadwick MB, Hughes HG, Little RC, Macfarlane RE, Waters LS, Young PG (2000) arXiv:nucl-th/00110666v117. Los Alamos National Laboratory, Nov 2000
34. Naik H, Prajapati PM, Suryanarayana SV, Jagadeesan KC, Thakare SV, Raj D, Mulik VK, Shivasahankar BS, Nayak BK, Sharma SC, Mukherjee S, Singh S, Goswami A, Ganesan S, Manchanda VK (2011) Eur. Phys. J A 47:51
35. The international Reactor Dosimetry File:IRDF-2002. Nuclear Data Section, International Atomic Energy Agency. http://www-nndc.bnl.gov/undoscr/libraries/irdf/
36. NuDat (BNL, USA) www.nndc.bnl.gov/nudat2/
37. Koning AJ, Hilaire S, Duijvestijn MC, TALYS-1.0., Proceedings of the International Conference on Nuclear Data for Science and Technology, April 22–27, 2007, Nice, France, Bersillon O, Gunsing F, Bauge E, Jacqmin R, Leray S (eds) EDP Sciences, 2008, p 211–214
38. Experimental Nuclear Reaction Data (EXFOR), Database Version of December 15, 2011, Software Version of 2011.11.17. http://www-nds.iaea.org/exfor/exfor.htm (IAEA); http://203.197.41.106/exfor/exfor.htm. Accessed 24 Jan 2012